JOURNAL OF MATERIALS SCIENCE 22 (1987) 601–606

# Shear band formation and cracking of a metallic glass irradiated with high energy laser pulses

K. MUKHERJEE, NARENDRA B. DAHOTRE, C. WAKADE
*Department of Metallurgy, Mechanics and Materials Science, Michigan State University, East Lansing, Michigan 48824, USA*

A concentric deformation pattern, shear bands and cracks are produced in $Fe_{80}B_{14.5}Si_{3.5}C_2$ glass, irradiated with 12 msec duration ruby laser pulses, ranging in power densities between $10^5$ and $10^7$ W cm$^{-2}$. This deformation front propagates through a steep temperature gradient and a partially crystallized heat-affected zone, giving rise to variations of the macroscopic deformation mode as a function of radial distance from the centre of the laser spot. For the first time, a direct experimental mapping of crack tip plasticity, in the form of an elliptical shear band zone, has been recorded. A theoretical model, which predicts such a shear band zone at the crack tip, is used to discuss the elastic–plastic response of the metallic glass.

## 1. Introduction

Interaction of a high energy pulse with a solid produces two nearly simultaneous effects: (i) a temperature spike within the irradiated volume and (ii) an elastic/plastic deformation front which propagates through the solid. The nature and magnitude of these two events depend on the thermophysical properties of the solid, input energy, spot size and energy–time profile of the laser pulse [1]. Highly localized thermal expansion, in the wake of a rapid heating pulse at the surface of an elastic solid, promotes a stress wave which propagates into the interior of the solid. The magnitude of the peak stress is a strong function of the pulse duration and for a pulse lasting a few nanoseconds, fracture and spallation is possible even in a very ductile metal [2]. Thus, laser processing, with high-energy pulse lasers, can produce adverse or undesirable side effects which must be carefully understood for a successful implementation of operations such as spot welding, surface hardening etc.

In this investigation, we have made an attempt to characterize thermomechanical processes associated with pulse laser interaction with thin foils of a metallic glass. The choice of this system results from the perceived need to spot-weld or join metallic glass foils in some specific engineering applications. Aside from this practical point of view, pulse laser interaction with a metallic glass and the associated physical and mechanical changes are of fundamental interest.

Unlike a crystalline metal or an alloy, the deformation mode in a metallic glass is primarily via the formation of shear bands, and the nature of strain localization and formation of shear bands in various metallic glasses have been studied extensively [3–19]. Both temperature and strain rate play important roles in controlling the nature of deformation in metallic glasses, and in a pulse-laser heated metallic glass foil the deformation proceeds through a steep temperature gradient. Thus, a complex transition of the deformation mode could be expected in the vicinity of an irradiated spot. Further, if the temperature of a region is $\geqslant T_g$, the glass transition temperature, then a partial crystallization of metallic glasses produces severe brittleness and therefore the laser-induced deformation can also produce cracks and fracture within the crystallized region. Shear band interaction with crystallites, in a partially crystallized metallic glass, has been studied [19] and these results might be applicable in the present case.

## 2. Experimental procedure

The metallic glass used in this investigation had a nominal composition of $Fe_{80}B_{14.5}Si_{3.5}C_2$. The thickness of the foil was 25 $\mu$m and the maximum lateral dimensions were 15 cm by 5 cm.

A pulse ruby laser was used in the normal mode to study the interaction mechanism. The laser could deliver a maximum energy of 150 J with a pulse duration of 12 msec. By focusing the laser beam to a spot diameter as small as 0.05 cm and using various neutral density filters, power density was varied from $\sim 10^5$ to $\sim 10^7$ W cm$^{-2}$.

Several hold-down conditions were utilized for this investigation. These included foils stretched as a membrane, foils supported on a metallic (conducting) or a glass (non-conducting) substrate. Further, some sample edges were sandwiched between two metallic flanges with circular O-rings. This latter method provided a well-defined circular boundary condition, the diameter of the O-ring being much larger than the spot size. Some samples were also irradiated through an optically flat quartz slide, sandwiching the sample against another non-conducting substrate.

## 3. Results and discussion

### 3.1. Hole formation and fracture

For a single foil of the metallic glass supported only along its edges, a circular hole was observed to form for a flux density of $\sim 10^7$ W cm$^{-2}$, as shown in Fig. 1. It must be noted that the hole diameter ($\sim 2500$ $\mu$m) is

0022–2461/87 $03.00 + .12 

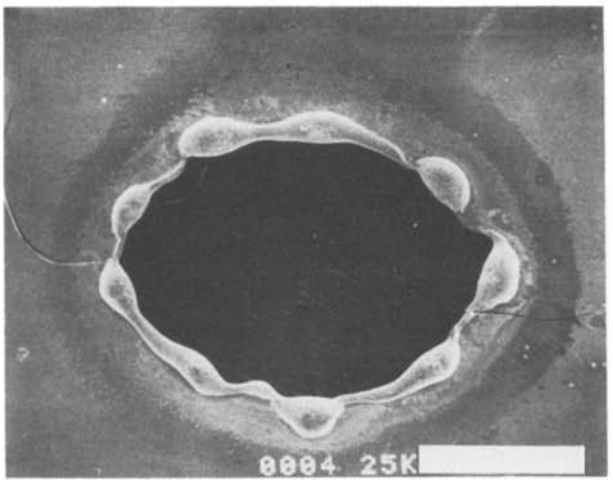


*Figure 1* Laser damage in a foil of metallic glass supported along its edges. Fluence $\sim 10^7\,W\,cm^{-2}$. Scale bar = 1000 $\mu$m.

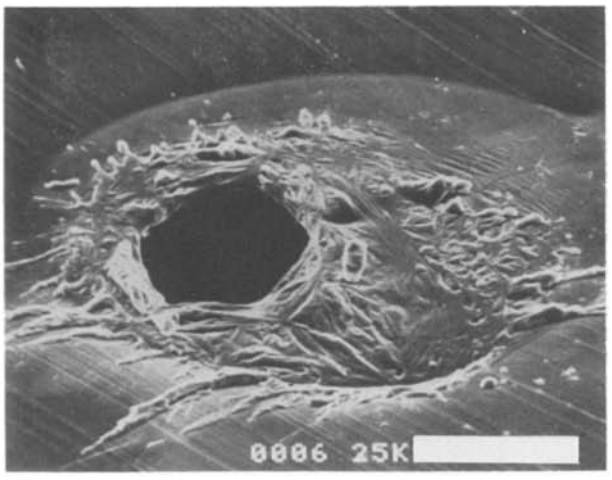


*Figure 2* Laser damage in aluminium foil. Fluence $\sim 10^7\,W\,cm^{-2}$. Spot size $\sim 500\,\mu m$. Scale bar = 100$\mu$m.

much larger than the spot size ($\sim 500\,\mu m$). This figure shows both a pair of radial cracks and a circumferential crack emanating from the resolidified lip of the hole. The nature of this damage site can be compared with the corresponding damage in a ductile and crystalline material subjected to the same flux density. For this purpose an aluminium foil of comparable thickness was used and the nature of damage in this material is shown in Fig. 2. The absence of any crack formation and profuse liquid metal ejection are noteworthy in this figure.

For the $Fe_{80}B_{14.5}Si_{3.5}C_2$ glass, on the other hand, very little liquid metal ejection is observed and a strong surface tension force has gathered the molten alloy in a well-defined lip. Also conspicuous are the cracks initiated from the lip region.

Figs 3a and b show the nature of the radial (R) and the circumferential (C) cracks. It is to be noted that the radial crack is a Mode I type (crack opening). It can be postulated that the Mode I cracks are produced by the contraction associated with the crystallization of the amorphous alloy. The free volume in the metallic glass is larger than the free volume (point defects) in a crystalline solid and thus upon crystallization void formation and/or contraction is expected [20]. The tearing type of cracks (Mode III) are observed to propagate well into the heat-affected zone. In many cases, the initial Mode I cracks are observed to make a transition to a Mode III nature during its propagation toward the heat-affected zone. It is known that the tearing energy for most metallic glasses is of the order of $10\,J\,cm^{-2}$ compared with about $0.01\,J\,cm^{-2}$ for a crystalline metal [20]. Thus, a tearing type of deformation is relatively difficult in such a material. It can be speculated, however, that the cracks are initiated by a crack-opening mode but propagated by a tearing mode, due to the severe elastic displacement normal to the foil plane produced by the laser shock wave. Such an elastic displacement of a metallic surface, due to a high energy laser pulse, has been reported by other investigators [2, 21].

## 3.2. Wavy deformation and shear band formation

The normal surface displacement, due to an elastic wave propagation, produces a concentric permanent plastic deformation in the foils. If the hold-down boundary condition is circular and symmetric to the laser spot, then a set of well-defined wavy deformation bands is observed as shown in Fig. 4. If the stored

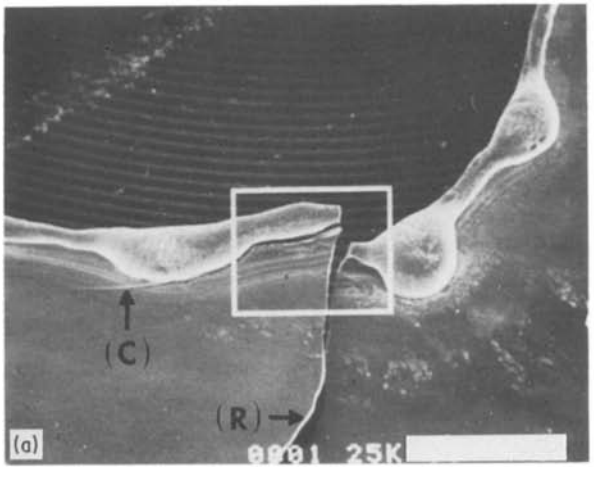


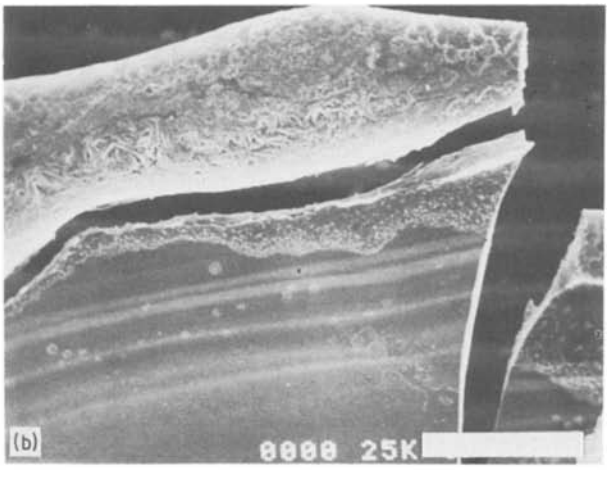


*Figure 3* (a) A low-magnification SEM micrograph showing crack formation. Radial cracks (R) and circumferential cracks (C) are marked by arrows. Scale bar = 600 $\mu$m. (b) Magnified view of the lip region from (a) showing concentric bands. Scale bar = 120 $\mu$m.

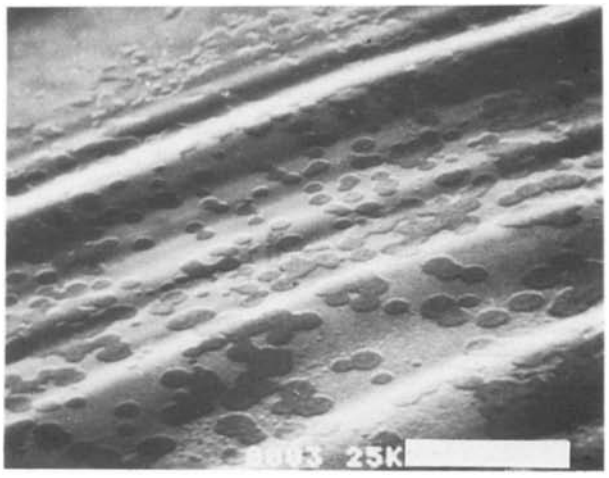

*Figure 4* SEM micrograph showing wavy deformation bands. Fluence $\sim 10^7\,W\,cm^{-2}$. Scale bar = 30 $\mu$m.

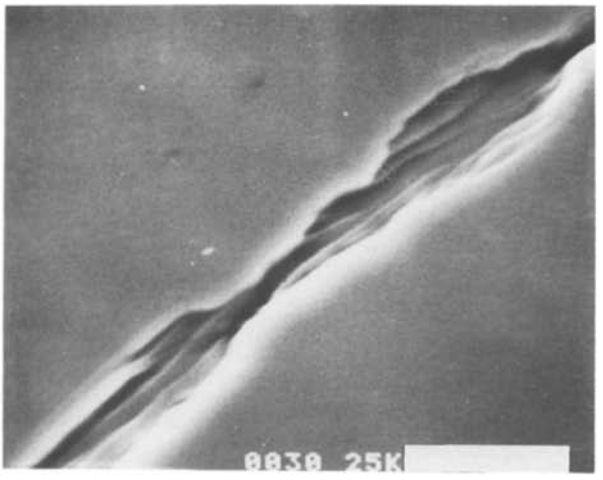

*Figure 6* Finer shear bands, $\sim 0.5\,\mu$m on the crack surface, away from the laser spot. Scale bar = 6 $\mu$m.

elastic energy in the propagating elastic wave front is sufficient to produce plastic deformation, then shear bands can form in such a material since shear band formation is the primary mode of yielding in metallic glasses.

The spacing of shear bands in a metallic glass is a function of temperature and the spacing is coarser at elevated temperatures [17]. Since the deformation, in our present examinations, occurs in a steep temperature gradient, it is expected that coarser bands will form near the laser spot and a finer band spacing will be found in regions away from the high-temperature zone. Indeed, this is found to be the case. Fig. 5 shows the relatively coarser shear band spacing on the crack surface near the lip of the hole. The average spacing in this region is $\sim 3\,\mu$m which can be compared with the shear band spacing of $\sim 0.5\,\mu$m on the crack surface away from the laser spot as shown in Fig. 6.

The nature of shear bands in the laser-damaged metallic glass is quite different from that produced by mechanical tearing of the foil at the ambient temperature. Fig. 7 shows the complex network of shear bands produced in our $Fe_{80}B_{14.5}Si_{3.5}C_2$ metallic glass by mechanical tearing at $\sim 295$ K. Such a generalized deformation was not observed during laser damage under any of the various sets of boundary conditions mentioned earlier.

It has been shown that the magnitude of the peak shock pressure is amplified if the surface of the metal is covered with a transparent overlay [2]. In our present case, a set of experiments was conducted in which the metallic glass foils were sandwiched between a quartz glass slide and a solid substrate. Aside from pressure amplification, the overlay also produced a constraint to the displacement normal to the foil plane. Tearing steps are now observed on the crack surface as shown in Figs 8a and b. A localized shear band formation, however, is observed at the crack tip (Fig. 8a) and this crack-tip plasticity will be discussed later.

### 3.3. Crack-tip plasticity

From the fracture mechanics point of view, crack problems in a hypothetical homogeneous, incompressible, isotropic, elastic material, have been recently considered by several investigators [22–24]. We note that an amorphous metallic glass satisfies these conditions more closely than a crystalline metal. Further, we consider a special class of materials which lose equilibrium ellipticity at sufficiently severe

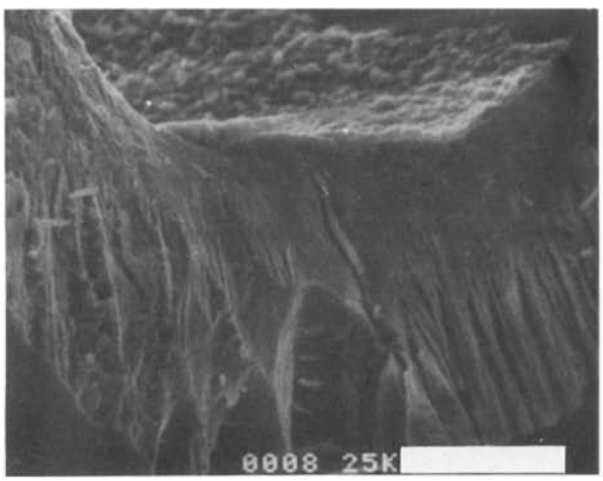

*Figure 5* Coarse shear bands on the fracture surface near the hole. Scale bar = 80 $\mu$m.

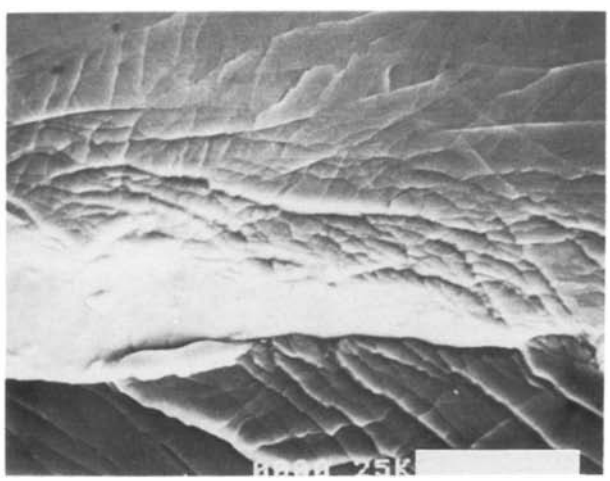

*Figure 7* Shear bands in the metallic glass produced by tearing. Scale bar = 15 $\mu$m.

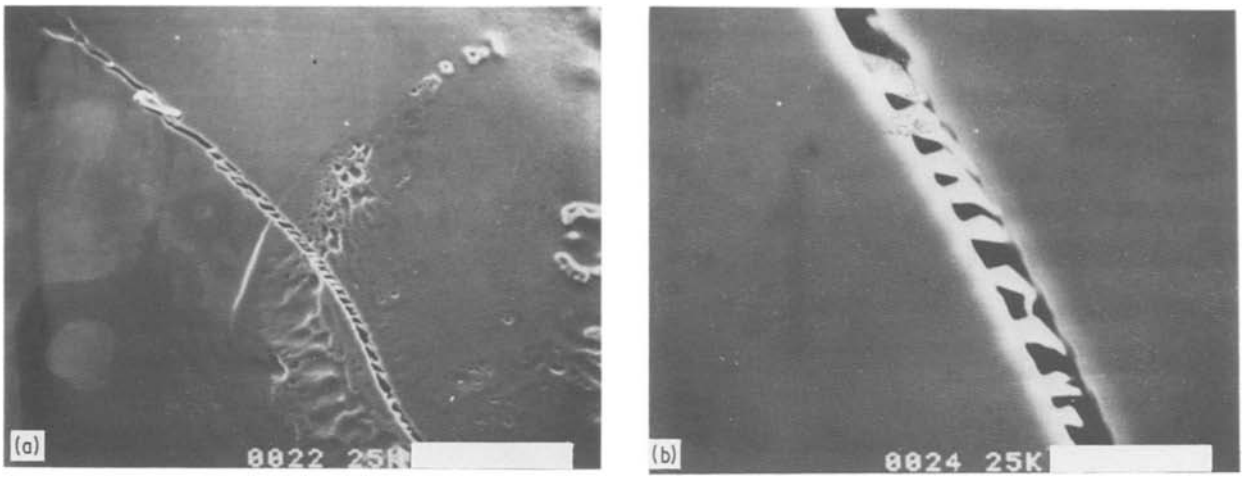


*Figure 8* (a) SEM micrographs showing tearing steps. Irradiation with a transparent overlay. Scale bar = 40 $\mu$m. (b) Magnified view of tear steps on the crack surface. Scale bar = 10 $\mu$m.

deformations. For this class of materials, the elastic field near a crack tip is quite different from that for materials which retain equilibrium ellipticity at all strains, e.g. most work-hardening metals and alloys without an yield drop. In these cases, the commonly considered point singularity at the crack tip is replaced by a finite singular domain. Instability, leading to shear band formation within this domain, is predicted from such a theory.

Most noteworthy results of this approach are predicted curves around a crack tip across which

(a) displacement and traction are continuous, but
(b) displacement gradient and stress suffer jump discontinuities.

The starting point for such a solution requires the assumption of a specific nature of the Cauchy shear stress–strain response curve of the material. One fundamental prerequisite for the hyperbolic solution near the crack tip is that at least one segment of the response curve exhibits a strain softening. Non-trivial solutions can then be obtained by considering the strain energy density function or the elastic potential, $W$. The authors [22–24] have considered

$$W = W(I_1) \tag{1}$$

where $I_1$ is the first fundamental scalar invariant of the Cauchy–Green deformation tensor. For an incompressible solid, the third scalar invariant, $I_3$; is unity and for the special class of material, $W$ is considered to be independent of the second invariant, $I_2$. For a Mode III crack problem, the out-of-plane displacement $U$ in the anti-plane shear field satisfies the differential equation

$$\nabla \cdot [W'(I_1) \nabla U] = 0 \tag{2}$$

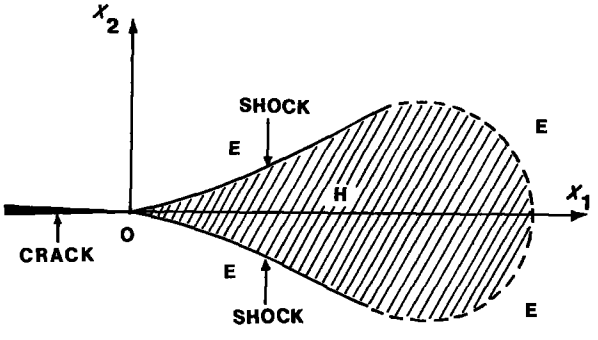


*Figure 10* Crack-tip plasticity corresponding to the response curve shown in Fig. 9 [22].

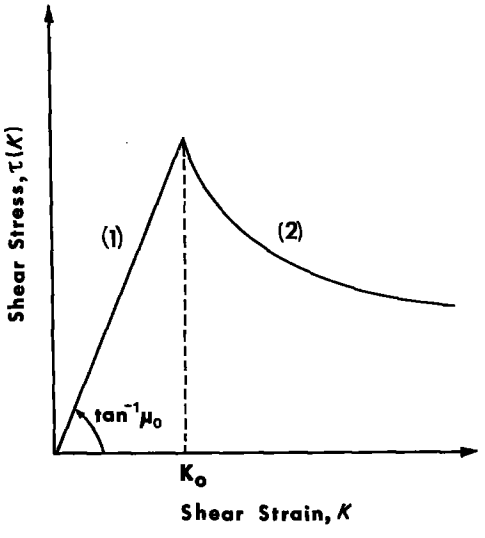


*Figure 9* Cauchy stress–strain curve assumed by Knowles and Sternberg [24].

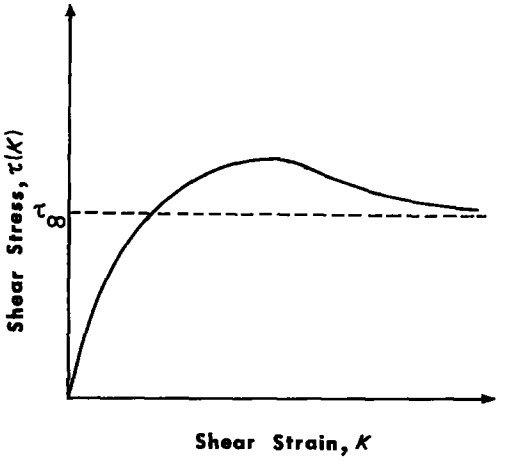


*Figure 11* A second type of stress–strain response curve assumed by Knowles and Sternberg. The response curve shows a maximum and a region of strain softening [24].

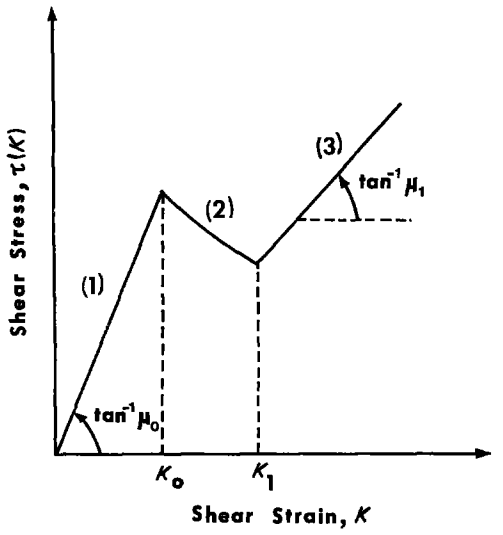


*Figure 12* Shear stress–strain curve of hypothetical solid assumed by Abeyaratne [23].

where $\nabla$ is the gradient operator and $W'$ is the derivative of $W$ with respect to $I_1$. Away from the crack tip, we have

$$I_1 = 3 + |\nabla U|^2 \tag{3}$$

At infinite distance, $U$ must correspond to that for a simple shear and thus

$$U \sim KX_2 \tag{4}$$

where $K \geqslant 0$ is the amount of applied shear and $X_2$ is along the coordinate normal to the direction of crack propagation and lies on the plane of the foil. Further, the traction on the faces of the crack must vanish. Equations 2 to 4, along with the vanishing traction at the crack faces, define a boundary-value problem.

Knowles [22], Knowles and Sternberg [24] and Abeyaratne [23] have solved this problem for various assumed shear stress, $\tau(K)$, and shear strain, $K$, response curves.

One of the response curves assumed by Knowles [22] is shown in Fig. 9. The segments (1) and (2) of this response curve are assumed to be given by

$$(1) \quad \tau(K) = \mu_0 K \qquad |K| \leqslant K_0 \tag{5}$$

$$(2) \quad \tau(K) = \mu_0 K^{-1/2} \qquad K_0 \leqslant |K| < \infty \tag{6}$$

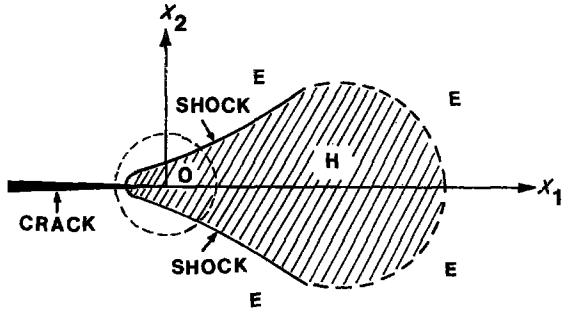


*Figure 13* Crack-tip plasticity corresponding to the response curve shown in Fig. 12. Shocks emanate from crack surface.

where $\mu_0$ is the slope of the linear segment and $K_0$ is defined in the diagram.

The corresponding crack-tip plasticity is shown by the schematic diagram in Fig. 10, as obtained by Knowles and Sternberg [24]. Across the hyperbolic (H) and elliptic (E) domain boundaries and across the elastostatic shocks, displacement and traction are continuous but displacement gradients and stress suffer a jump discontinuity. Within the cross-hatched region, therefore, strain localization and shear band formation is predicted.

A second type of response curve [24] is shown in Fig. 11. In this case, no explicit expression for $\tau(K)$ is assumed. The corresponding elliptic and hyperbolic regions in this case are similar to those shown in Fig. 10 except for the fact that the angle of the shock curves approaching the crack tip is modified by the magnitude of $\tau_\infty$. The most important feature of these solutions which is relevant to our present discussions is that the shear band zone emanates from the crack tip.

A third type of response curve due to Abeyaratne [23] is shown in Fig. 12, in which the three segments are represented by

$$(1) \quad \tau(K) = \mu_0 K \qquad |K| \leqslant K_0 \tag{7}$$

$$(2) \quad \tau(K) = \mu_0 K_0^{3/2} K^{-1/2} \qquad K_0 \leqslant |K| \leqslant K_1 \tag{8}$$

$$(3) \quad \tau(K) = \mu_1 K + (\mu_0 K_0^{3/2} - \mu_1 K_1^{3/2})/K_1^{1/2} \qquad |K| \geqslant K_1 \tag{9}$$

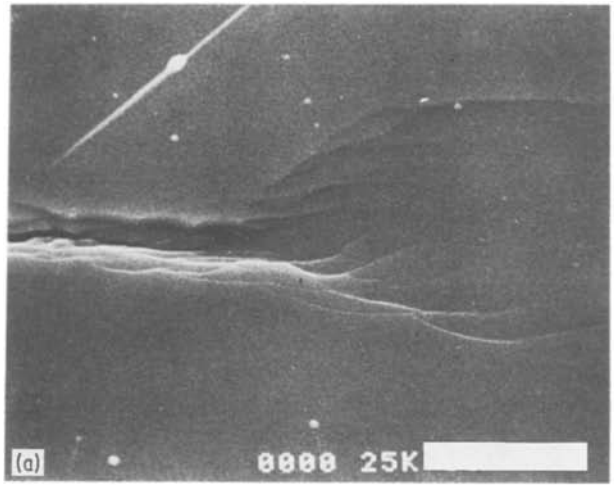


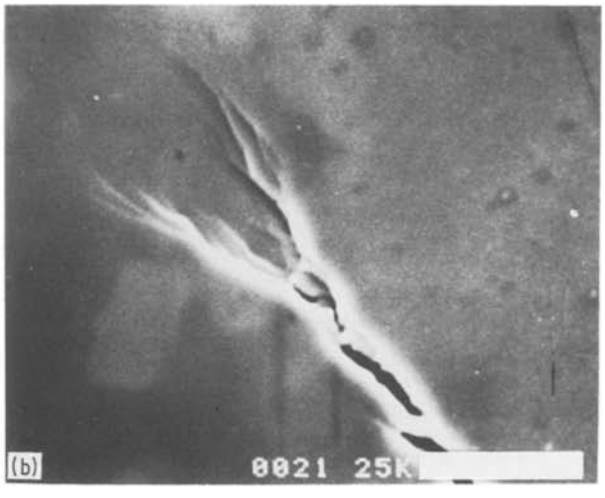


*Figure 14* (a) Elliptical shear band zone at the crack tip. Fluence $\sim 10^7\,\mathrm{W\,cm^{-2}}$; scale bar = 6 $\mu$m. (b) Crack-tip plasticity induced by laser damage in a metallic glass with transparent overlay; scale bar = 10 $\mu$m.

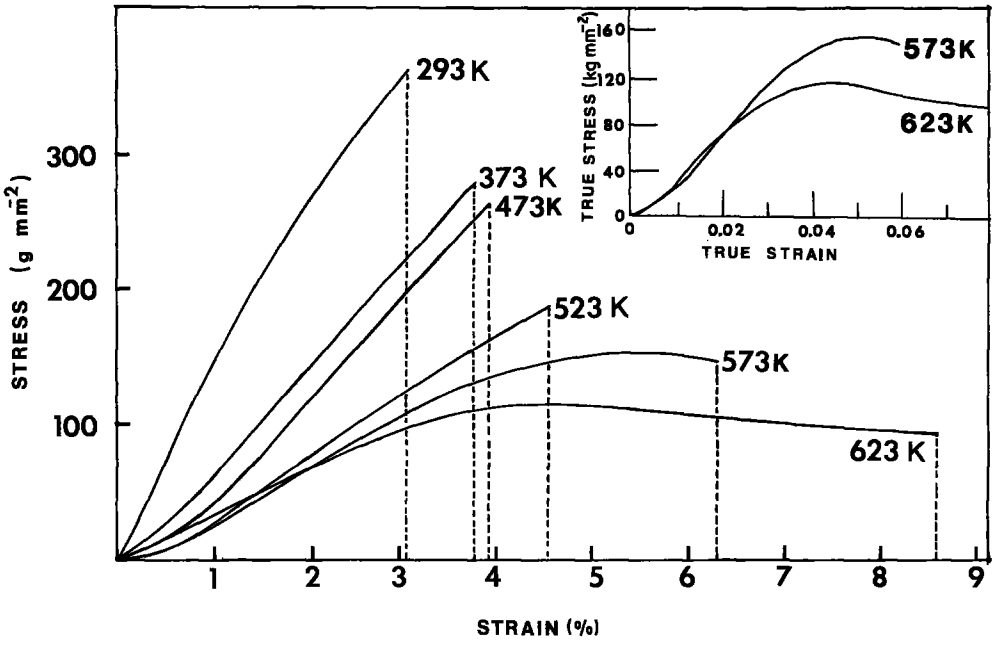


*Figure 15* Stress–strain response of $Fe_{80}B_{14.5}Si_{3.5}C_2$ alloy as a function of test temperature. Curve for 573 K could be compared with Fig. 11.

The solution for this case is shown schematically in Fig. 13. The relevant feature of this solution is that the shear band could start from the crack surface behind the crack tip.

Returning now to our experimental results, we present the evidence of crack-tip plasticity in the form of a shear band zone. Fig. 14 shows such a shear band configuration at the crack tip. This figure is remarkably similar to the theoretically predicted configuration as shown in Fig. 10, i.e. the shear band emanates from the crack tip.

Unfortunately, we do not have the shear stress–strain response curve for the $Fe_{80}B_{14.5}Si_{3.5}C_2$ alloy. However, we note that the tensile stress–strain response of a metallic glass is sensitive to test temperature as has been shown by Masumoto and Maddin [3]. Fig. 15 shows such a set of tensile response curves of metallic glass $Fe_{80}B_{14.5}Si_{3.5}C_2$ as a function of test temperature. The curve at 573 K is not unlike the schematic response curve (Fig. 11) assumed by Knowles and Sternburg [24]. The strain softening behaviour seems to exist, in this alloy, at temperatures above 523 K. Since the crack propagation in the laser pulsed material proceeds through a steep temperature gradient, a crack-tip shear band zone is possible when the crack arrest occurs in a region where the temperature is suitable for such an instability. To the best of our knowledge, this is the first experimental evidence of a mapping of the crack tip plasticity in accordance with the theoretical prediction.

## Acknowledgements

The authors would like to thank Dr H. H. Liebermann of the Metglas Products Department of the Allied Corporation (Parsippany, New Jersey) for providing samples of $Fe_{80}B_{14.5}Si_{3.5}C_2$ used in this research. The authors would like to thank Professor R. Abeyaratne for introducing theory to the literature on crack tip plasticity.

## References

1. J. F. READY, "Effects of High-Power Laser Radiation" (Academic Press, New York, 1971) pp. 357–396.
2. K. MUKHERJEE, T. H. KIM and W. T. WALTERS, in "Lasers in Metallurgy", edited by K. Mukherjee and J. Majunder (The Metallurgical Society of AIME, Warrendale, Pennsylvania, 1981) pp. 137–150.
3. T. MASUMOTO and R. MADDIN, *Acta Metall.* **19** (1971) 725.
4. H. J. LEAMY, H. S. CHEN and T. T. WANG, *Met. Trans.* **5** (1972) 699.
5. C. A. PAMPILLO and A. C. REIMSCHUESSEL, *J. Mater. Sci.* **9** (1974) 718.
6. S. TAKAYAMA and R. MADDIN. *Met. Trans.* **7A** (1976) 1065.
7. L. A. DAVIS and S. KAVESJ, *J. Mater. Sci.* **10** (1975) 453.
8. F. SPAEPEN, *Acta Metall.* **25** (1977) 407.
9. H. NEUHAUSER, *Scripta Metall.* **12** (1978) 471.
10. A. S. ARGON, *Acta Metall.* **27** (1979) 47.
11. S. TAKAYAMA, *Scripta Metall.* **15** (1979) 463.
12. A. I. TAUB, *Acta Metall.* **28** (1980) 633.
13. P. E. DONOVAN and W. M. STOBBS, *ibid.* **29** (1981) 1419.
14. P. S. STEIF, F. SPAEPEN and J. W. HUTCHINSON, *ibid.* **30** (1982) 447.
15. L. A. DAVIS, *Scripta Metall.* **16** (1982) 993.
16. A. S. ARGON and L. T. SHI, *Acta Metall.* **31** (1983) 499.
17. P. E. DONOVAN and W. M. STOBBS, *ibid.* **31** (1983) 1.
18. H. KIMURA and T. MASUMOTO, *ibid.* **31** (1983) 240.
19. P. E. DONOVAN and W. M. STOBBS, *J. Non-Cryst. Solids* **55** (1983) 61.
20. H. S. CHEN, *Rep. Prog. Phys.* **43** (1983) 353.
21. R. M. WHITE, *J. Appl. Phys.* **34** (1964) 2123.
22. J. K. KNOWLES, in Proceedings of the IUTAM Symposium on Finite Elasticity, Lehigh University, 1980, edited by D. E. Carlson and R. T. Shield (Martinus Nijhoff, The Hague, 1982) p. 257.
23. R. ABEYARATNE, *J. Elasticity* **11** (1981) 373.
24. J. K. KNOWLES and E. STERNBERG, *ibid.* **11** (1981) 129.

*Received 4 April*
*and accepted 5 June 1986*